Development 139, 2040-2049 (2012) doi:10.1242/dev.074054

Nf1 limits epicardial derivative expansion by regulating epithelial to mesenchymal transition and proliferation

Seung Tae Baek and Michelle D. Tallquist*

SUMMARY

The epicardium is the primary source of coronary vascular smooth muscle cells (cVSMCs) and fibroblasts that reside in the compact myocardium. To form these epicardial-derived cells (EPDCs), the epicardium undergoes the process of epithelial to mesenchymal transition (EMT). Although several signaling pathways have been identified that disrupt EMT, no pathway has been reported that restricts this developmental process. Here, we identify neurofibromin 1 (Nf1) as a key mediator of epicardial EMT. To determine the function of Nf1 during epicardial EMT and the formation of epicardial derivatives, cardiac fibroblasts and cVSMCs, we generated mice with a tissue-specific deletion of *Nf1* in the epicardium. We found that mutant epicardial cells transitioned more readily to mesenchymal cells in vitro and in vivo. The mesothelial epicardium lost epithelial gene expression and became more invasive. Using lineage tracing of EPDCs, we found that the process of EMT occurred earlier in *Nf1* mutant hearts, with an increase in epicardial cells entering the compact myocardium. Moreover, loss of Nf1 caused increased EPDC proliferation and resulted in more cardiac fibroblasts and cVSMCs. Finally, we were able to partially reverse the excessive EMT caused by loss of Nf1 by disrupting Pdgfrα expression in the epicardium. Conversely, Nf1 activation was able to inhibit PDGF-induced epicardial EMT. Our results demonstrate a regulatory role for Nf1 during epicardial EMT and provide insights into the susceptibility of patients with disrupted NF1 signaling to cardiovascular disease.

KEY WORDS: Neurofibromin 1, Epicardium, EMT, EPDC, Mouse

INTRODUCTION

The epicardium, which comprises the outer epithelial layer of the heart, is a cell population that undergoes epithelial to mesenchymal transition (EMT) during development (Lie-Venema et al., 2007). Around embryonic day (E) 13.5, a subset of epicardial cells lose their epithelial characteristics, gain mesenchymal properties and migrate into the heart to differentiate into coronary vascular smooth muscle cells (cVSMCs) and cardiac fibroblasts (Dettman et al., 1998; Manner et al., 2001; Mikawa and Gourdie, 1996). Several growth factors, including transforming growth factor β (TGFβ) (Mercado-Pimentel and Runyan, 2007; Xu et al., 2009b) and fibroblast growth factor (FGF) (Pennisi and Mikawa, 2009) have been implicated in the EMT process of epicardial cells during heart development, but little is understood about signals that limit the EMT process. Identification of such pathways will provide insights into the complex regulation of EMT during heart development. Because many of these same signaling pathways have also been suggested to play a key role in cardiac fibrosis, this might also provide insights into pathological EMT.

Recent findings show that disruption of Ras-mitogen activated protein kinase (MAPK) signaling results in several syndromes that exhibit congenital heart defects, including the Costello (Aoki et al., 2005), LEOPARD (Kontaridis et al., 2006), cardio-facio-cutaneous (Niihori et al., 2006) and Noonan (Schubbert et al., 2006) syndromes. Loss of neurofibromin 1 (Nf1; also known as neurofibromatosis-related protein NF-1), a Ras-GTPase activating protein (GAP), leads to hyperactivation of Ras and its downstream components (Cichowski and Jacks, 2001; Martin et al., 1990; Xu et al., 1990). Although mutations in *NF1* are best known for causing neurofibromatosis type 1 tumors of the skin and nervous system (Lynch and Gutmann, 2002), patients with *NF1* mutations also have an increased risk for cardiovascular disorders (Lin et al., 2000).

Studies in mice have significantly advanced our understanding of Nf1 function during heart development. Inactivation of *Nf1* causes lethality at mid-gestation, with severe heart defects including malformation of the outflow tract, a thinned myocardium, a ventricular septal defect and enlarged endocardial cushions (Brannan et al., 1994; Jacks et al., 1994). Loss of *Nf1* in vascular smooth muscle cells (VSMCs) leads to an abnormal proliferative injury response (Xu et al., 2007), and cardiomyocyte-specific inactivation of *Nf1* results in pathological hypertrophy and heart failure in adult mice (Xu et al., 2009a). *Nf1*-null endocardial cushion cells exhibit abnormal EMT (Lakkis and Epstein, 1998), and endothelial-specific deletion of *Nf1* recapitulates many of the cardiovascular defects of the *Nf1*-null mouse, suggesting an indispensable role of Nf1 in endothelial cells during EMT (Gitler et al., 2003).

We have investigated the function of Nf1 in epicardial development using *Cre/loxP* technology to inactivate *Nf1* in the mouse epicardium. We found that loss of Nf1 results in increased EMT and epicardial-derived cell (EPDC) proliferation, leading to a substantial expansion of this cell population that includes cardiac fibroblasts and cVSMCs. Our data point to a regulatory role for Nf1 in the process of EMT and suggest the possibility that patients with disruption of *NF1* might be more prone to cardiac complications such as fibrosis and coronary artery disease.

MATERIALS AND METHODS

Mice

Mice were maintained on a mixed C57/BL6 × 129SV background. Mice with the *Gata5-Cre* transgene (Merki et al., 2005) or $Wt1^{GFPCre}$ allele (Zhou et al., 2008) were crossed with mice with the *Nf1* floxed ($Nf1^{fl}$) allele (Zhu et al., 2001) to generate $Nf1^{fl/fl}$;$Gata5\text{-}Cre^{Tg}$ (designated $Nf1^{G5KO}$) and

Department of Molecular Biology, University of Texas Southwestern Medical Center, Dallas, TX 75390-9148, USA.

*Author for correspondence (michelle.tallquist@utsouthwestern.edu)

Accepted 27 March 2012

Nf1$^{fl/fl}$;*Wt1*^{GFPCre}, respectively. Controls were *Cre*-negative littermates (*Nf1*$^{fl/fl}$ or *Nf1*$^{fl/+}$) unless otherwise indicated. For epicardial tracing experiments, male *Nf1*$^{fl/+}$;*Wt1*$^{CreERT2/+}$ mice were crossed with *Nf1*$^{fl/fl}$ or *Nf1*$^{fl/+}$ female mice with *ROSA26R*^{lacZ} (designated *R26R*^{lacZ}) (Soriano, 1999) or *ROSA26R*^{tdTomato} (designated *R26R*^{T}) (Madisen et al., 2010) reporter alleles to generate *Nf1*$^{fl/fl}$;*Wt1*$^{CreERT2/+}$ (designated *Nf1*^{WTiKO}). *Wt1*^{CreERT2} was induced by oral administration of tamoxifen (MP Biomedicals, 02156738) to pregnant females at the indicated embryonic stages and induction efficiency was traced by *R26R*^{lacZ} or *R26R*^{T} reporter gene expression. Tamoxifen was dissolved in sunflower seed oil (Sigma) at 20 mg/ml and administrated at a final concentration of 0.1 mg per gram body weight. Other strains in these experiments include *Pdgfra*^{fl} (Tallquist et al., 2003) and *K-Ras(G12D)*^{fl} mice (JAX stock number 008180) (Jackson et al., 2001). All animal protocols were approved by the Institutional Animal Care and Use Committee of the University of Texas Southwestern Medical Center and conform to NIH guidelines for care and use of laboratory animals. *Nf1*^{fl} (Zhu et al., 2001) and *Gata5-Cre*^{Tg} (Merki et al., 2005) mice were kindly provided by Dr Luis Parada (University of Texas Southwestern, TX, USA) and Dr Pilar Ruiz-Lozano (Sanford-Burnham Institute, CA, USA), respectively. *Wt1*^{GFPCre} and *Wt1*^{CreERT2} mice (Zhou et al., 2008) were kindly provided by Dr William Pu (Harvard, MA, USA) and *X-LacZ4*^{Tg} mice (Tidhar et al., 2001) were kindly provided by Dr Moshe Shani (Volcani Center, Israel).

Primary epicardial cultures

In vitro culture of epicardial cells was described previously (Mellgren et al., 2008). Ventricles from E12.5 hearts were isolated and cultured in 1:1 DMEM:M199 with 15% FBS supplemented with glutamate, antibiotics and basic fibroblast growth factor (2 ng/ml, Sigma). After 3 days, heart explants were removed and cells were cultured for 2 additional days in media with reduced serum (10%). The epicardial nature of the culture was confirmed by the expression of epicardial gene reporters: *Tcf21*^{lacZ} (Lu et al., 1998) or *Pdgfra*^{GFP} (Hamilton et al., 2003; Smith et al., 2011) (data not shown). Cre-expressing adenovirus, kindly provided by Dr Robert Gerard, University of Texas Southwestern, TX, USA), was added to the culture as indicated. For RNA extraction followed by quantitative real-time PCR (qRT-PCR) analysis, hearts were cultured in 24-well plates. Loss of *Nf1* in *Nf1*^{G5KO} cultures was confirmed by qRT-PCR. For immunostaining, hearts were placed on glass coverslips coated with collagen type IV (5 μg/cm^2, R&D Systems). Collagen-coated coverslips were prepared according to the manufacturer's protocol. For the in vitro differentiation assay, epicardial cells were cultured for a total of 6 days followed by immunostaining.

Tissues, staining and immunostaining

Tissues and embryos were fixed in 4% paraformaldehyde (PFA) overnight at 4°C, washed in PBS, dehydrated and paraffin embedded. For histological analysis, tissues were sectioned to 8 μm, rehydrated and stained with Hematoxylin and Eosin (Sigma) as previously described (Mellgren et al., 2008). For immunostaining, antigens were retrieved in citrate buffer (pH 6.0) at 98°C for 15 minutes using a temperature-controlled microwave (BioGenex). For frozen embedding, hearts were fixed in 4% PFA for 1 hour at 4°C then embedded in OCT (Tissue-Tek). Hearts were sectioned at 10 μm, permeabilized with 0.1% Triton X-100 in PBS (PBT), blocked with 5% serum in PBT and stained with phalloidin (1:200; Invitrogen, A12379) or with antibodies against vimentin (1:500; Sigma, V6630), SM-MHC (1:250; Chemicon, MAB3572), phospho-histone H3 (1:200; Upstate, 06-570), collagen IV (1:250; Chemicon, AB748), β-catenin (1:500; BD Bioscience, 610153) and α-catenin (1:100; Abcam, AB51032). Immunostaining for Wt1 (1:50; DAKO, M3561) was performed with the Vectastain mouse ABC kit followed by detection by DAB (Vector Labs).

For the detection of β-galactosidase activity, hearts were fixed in 2% formaldehyde/0.2% glutaraldehyde in PBS for 15 minutes. Hearts were then washed with PBS and stained whole-mount with X-Gal (Gold Biotechnology, X4281C) or frozen embedded and sectioned, followed by staining as described previously (Acharya et al., 2011).

Whole-mount confocal imaging

For whole-mount immunostaining, hearts were isolated and fixed in 4% PFA, then permeabilized with PBT for 30 minutes, blocked with CAS Block (Invitrogen, 008120) for 30 minutes, and immunostained for β-catenin (1:200). *z*-stack images (nine consecutive 4 μm images spanning 32 μm in depth) were taken from similar regions of the left ventricle of embryonic hearts starting from the epicardial surface using an LSM 510 META mounted on an Axiovert 200M fluorescence microscope (Zeiss). Three-dimensional images were reconstituted using ImageJ software, and the total number of cells expressing R26R^{T} within a 150 μm × 150 μm × 32 μm area were counted in the subepicardial space.

Collagen gel invasion assay

The collagen gel invasion assay was performed as described (Boyer et al., 1999; Potts et al., 1991) with modifications. E12.5 hearts were isolated, and ventricles were placed and cultured on 1.6% collagen (Roche) gels. Collagen gels were prepared according to the manufacturer's instructions. After 3 days, heart explants were removed and cultured for 3 more days before fixing in 4% PFA for 10 minutes for analysis. To detect invasion, collagen gels were frozen embedded and sectioned, followed by staining with DAPI (Roche) and phalloidin. Invasion was identified by the presence of epicardial cells underneath the collagen gel surface. For quantification, invading cells were identified using a fluorescence microscope (Zeiss Axiovert 200M with a Hamamatsu ORCA-ER camera) and invasion was calculated by imaging from the center of each culture along a line to where cells had left the plane of the collagen gel (the invasion front). For quantification, the number of cells that had invaded the gel was divided by the total number of cells within the 20× field of view from three different images (Merki et al., 2005).

Ex vivo migration assay

The ex vivo migration assay was performed as described (Mellgren et al., 2008). E12.5 hearts were isolated and incubated with adenovirus expressing GFP or Nf1 GAP-related domain (Miller et al., 2010), kindly provided by Dr Robert Gerard or Dr Nancy Ratner (Cincinnati Children's Hospital, OH, USA), respectively. PDGF-BB (R&D Systems), imatinib mesylate (Sigma), AG1296 (Sigma) and U0126 (Sigma) were added to the cultures as indicated. After 2 days, hearts were fixed in 4% PFA and frozen embedded, sectioned and stained for DAPI. For quantification, GFP^{+} cells underneath the epicardium were counted in a 40× field of view from five nonconsecutive sections.

Quantification and statistical analysis

For mesenchymal index, primary cultured epicardial cells were stained for β-catenin and phalloidin as described above, and cells exhibiting a mesenchymal morphology were identified by the loss of adherens junctions and cortical actin and by the robust formation of actin stress fibers (Sridurongrit et al., 2008). Mesenchymal cells were counted and divided by the total number of cells in a 40× field of view from three different regions of the cultures. β-galactosidase staining was quantified as previously described (Morgan et al., 2008). Epicardial differentiation of smooth muscle cells was quantified following immunostaining against SM-MHC. The SM-MHC-positive area was measured and divided by the DAPI positive area in three 40× field-of-view images using ImageJ (NIH). All experiments used a minimum of two independent litters, and data were analyzed by Student's *t*-test using Prism 5 (GraphPad Software).

qRT-PCR

Primary epicardial cells were collected as described above. RNA isolation and cDNA synthesis were as described previously (Mellgren et al., 2008) with slight modifications. Briefly, primary epicardial cultures from three hearts of each genotype were combined followed by RNA isolation using Trizol (Invitrogen). cDNA was synthesized using Superscript III reverse transcriptase (Invitrogen). Gene transcription was analyzed by standard qRT-PCR with iTAQ SYBR Green Master Mix (Bio-Rad) using the CFX96 real-time PCR detection system (Bio-Rad). Each sample was run in triplicate. Sequences of primers are as reported previously (Smith et al., 2011).

In situ hybridization on tissue sections

Section in situ hybridization was performed as described previously (Schaeren-Wiemers and Gerfin-Moser, 1993; Smith et al., 2011). Briefly, embryonic hearts were isolated, fixed in 4% PFA, frozen embedded and

sectioned at 16 μm. Sections were digested with proteinase K (15 μg/ml; Fisher Scientific, BP1700-100) followed by brief fixation with 4% PFA and acetylation by acetic anhydride before hybridizing with digoxigenin-labeled RNA probes for *Pdgfra* (Bostrom et al., 1996), *Col1a1*, *Col3a1* and *Nf1*. Sections were then immunostained for digoxigenin (1:2000; Roche, 11093274910) followed by development with BM purple (Roche, 11442074001). Plasmids for *Col1a1* and *Col3a1* probes were kindly provided by Benoit de Crombrugghe (MD Anderson Cancer Center, TX, USA). The plasmid for the *Nf1* probe included a 338 bp fragment of the *Nf1* 3′ untranslated region corresponding to positions 9881-10,218 (GenBank L10370.1).

RESULTS

Epicardial inactivation of *Nf1* results in aberrant epicardium development

Loss of *Nf1* in cardiomyocytes or the endocardial cushions results in heart abnormalities (Gitler et al., 2003; Xu et al., 2009a), but no reports have addressed the disrupted epicardium observed in *Nf1*-null hearts (Brannan et al., 1994). To determine whether *Nf1* has a primary role in epicardial development, we performed in situ hybridization for *Nf1* transcripts. *Nf1* expression was detected in the epicardium, endocardium, endocardial cushions and myocardium at E11.5, but by E12.5 myocardial expression was decreased (supplementary material Fig. S1). Epicardial expression continued until E13.5, but by E14.5-15.5 was limited to a few cells in the epicardium (Fig. 1A; supplementary material Fig. S1).

To investigate Nf1 function in epicardial development, we initially used two mouse lines with constitutive expression of Cre in the epicardium: the *Gata5-Cre*^{Tg} (Merki et al., 2005) and the *Wt1*^{GFPCre} (Zhou et al., 2008) mouse lines. We monitored loss of *Nf1* transcript by *Gata5-Cre*^{Tg}-driven recombination (referred to as *Nf1*^{G5KO}) and found little expression in the epicardium and endocardial cushions at E13.5 (Fig. 1B). Using Wt1 protein expression to track the epicardium and undifferentiated EPDCs (Moore et al., 1999) we found that, unlike control hearts in which Wt1^{+} cells were restricted to the epicardium at E12.5, Wt1^{+} cells in *Nf1*^{G5KO} hearts were detected in not only the epicardium but also the subepicardial zone (Fig. 1C). To determine whether these cells had adopted a mesenchymal phenotype, we stained for vimentin, a marker for mesenchymal cells that often indicates that a cell has undergone the process of EMT (Perez-Pomares et al., 1997). At E12.5, control hearts had few vimentin^{+} cells in the subepicardium (Fig. 1D), whereas in *Nf1*^{G5KO} hearts there were multiple patches of vimentin^{+} cells in the subepicardium. These patches were often concomitant with a disrupted basement membrane (collagen IV staining; Fig. 1D). Similar patches of vimentin^{+} cells were also found when *Nf1* expression was disrupted using a *Wt1*^{CreGFP} allele for recombination (Fig. 1D).

Based on ROSA26 reporter activity, both of these epicardial Cre lines recombine in a significant number of cardiomyocytes and in the endocardial cushions (data not shown). Therefore, we performed the remaining in vivo experiments employing the

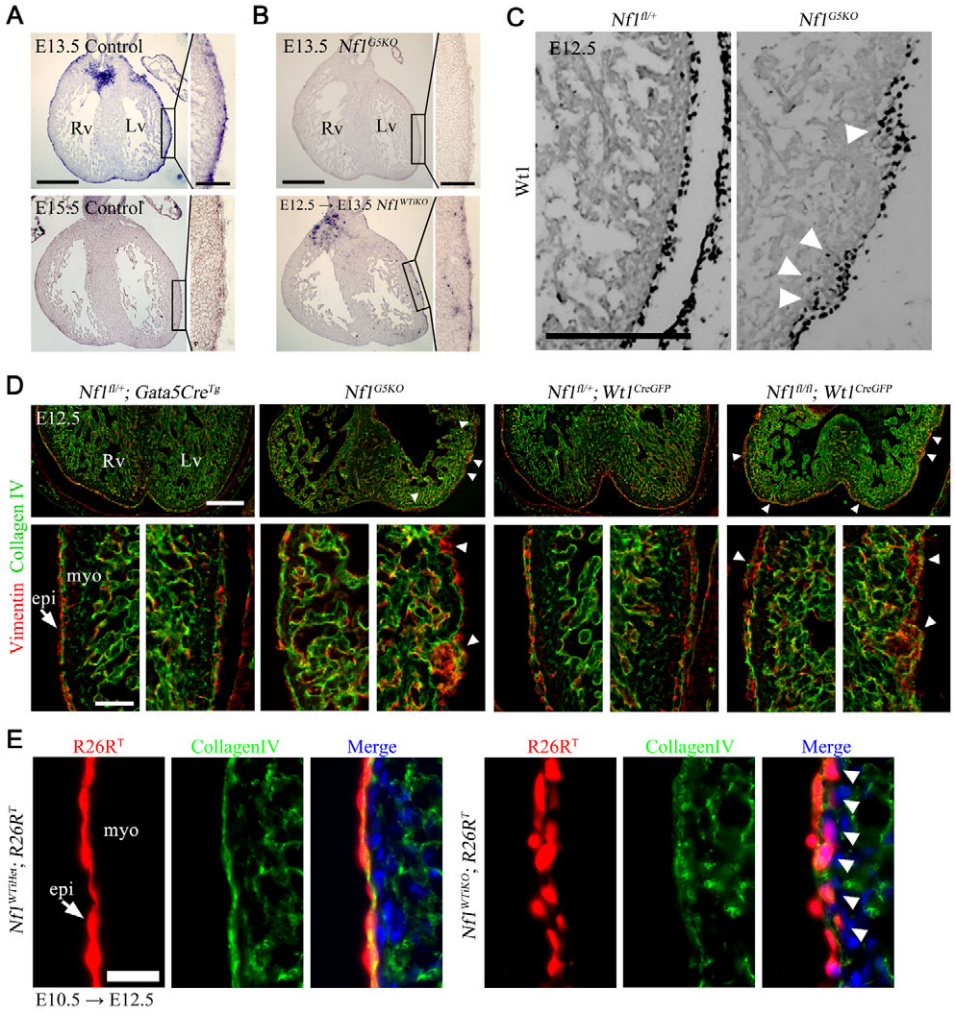

Fig. 1. Disruption of epicardial development by loss of Nf1 in epicardium. (**A**,**B**) *Nf1* mRNA expression was detected by in situ hybridization in heart sections of the indicated genotype. *Nf1*^{WTiKO} mouse embryos were maternally induced with tamoxifen for Cre activity at E12.5 for 24 hours before processing (E12.5 → E13.5). The boxed regions are shown at higher magnification in the insets. (**C**) Immunohistochemistry (IHC) for the epicardial marker Wt1. Arrowheads indicate increased invasion of Wt1^{+} cells. (**D**) IHC for vimentin and collagen IV in embryonic hearts of the indicated genotype. Arrowheads indicate expansion of epicardial cells into the subepicardium. Bottom panels are higher magnifications of left and right ventricle. Arrow indicates epicardium. (**E**) R26R^{T} fluorescence in heart sections of the indicated genotype. Oral tamoxifen administration is indicated by the stage of administration followed by the stage of isolation (E10.5 → E12.5). Arrows indicate epicardium. Arrowheads indicate migrated epicardial cells (below the basement membrane, collagen IV). Rv, right ventricle; Lv, left ventricle; epi, epicardium; myo, myocardium. Scale bars: 500 μm in A,B; 100 μm in A,B insets; 200 μm in C,D top; 50 μm in D bottom; 25 μm in E.

inducible epicardial-specific Cre mouse *Wt1*^{CreERT2} (Zhou et al., 2008). First, we confirmed the fidelity of recombination in this line to demonstrate epicardial-specific Cre activity with tamoxifen induction at E10.5 and E12.5. Single administration of tamoxifen at E10.5 resulted in reporter gene (*R26R*^{T}) expression in ~95% of epicardial cells after 24 hours (data not shown). Lineage tracing and in situ hybridization for *Nf1* demonstrated that in *Nf1* conditional embryos transcripts were reduced in the epicardium just 24 hours after induction (Fig. 1B), that epicardial cells were exclusively tagged, and that lineage-tagged cells migrated into the heart ventricles as expected (supplementary material Fig. S2A). The only other lineage-tagged regions were the atrioventricular valves, where epicardial cell contribution has been reported previously (de Lange et al., 2004). By contrast, at these time points of induction no lineage-tagged cells were detected in the cardiomyocyte population, nor in the semilunar valves (supplementary material Fig. S2B,C).

To specifically examine the role of Nf1 in the epicardium, we generated *Nf1*$^{fl/fl}$;*Wt1*$^{CreERT2/+}$ mice (referred to as *Nf1*^{WTiKO}). We obtained the expected Mendelian ratios of animals and detected no overt phenotype in *Nf1*^{WTiKO} animals, suggesting that epicardial inactivation of *Nf1* by *Wt1*^{CreERT2} at E12.5 did not cause embryonic nor postnatal lethality (data not shown). Because we observed vimentin^{+} cells in the ventricles at time points earlier than expected (Fig. 1D), we examined whether premature EMT occurred upon loss of Nf1 by tracing the migration of epicardial cells labeled at E10.5. These hearts revealed that a substantial number of epicardial cells were present immediately below the basement membrane in *Nf1*^{WTiKO} hearts, whereas tagged cells remained in the epicardium in controls (Fig. 1E). These data suggested that, in the absence of Nf1, epicardial cells migrate into the heart earlier than expected in all three genotypes examined (*Nf1*^{G5KO}, *Nf1*$^{fl/fl}$;*Wt1*$^{CreGFP/+}$ and *Nf1*^{WTiKO}).

Loss of Nf1 results in spontaneous EMT of epicardial cells in vitro

From the above data, we hypothesized that loss of Nf1 could result in accelerated EMT. First, we tested this possibility in vitro. We generated primary cultured epicardial cells from E12.5 hearts, which uniformly expressed the epicardial genes *Tcf21* and *Pdgfra* (data not shown). After 3 days of culture, without any exogenous stimulus the control epicardial cells remained a cobblestone monolayer, whereas *Nf1*^{G5KO} epicardial cells exhibited a mesenchymal morphology (Fig. 2A). We investigated two hallmarks of EMT, namely the loss of cell-cell contacts and the formation of actin stress fibers, by localization of β-catenin and

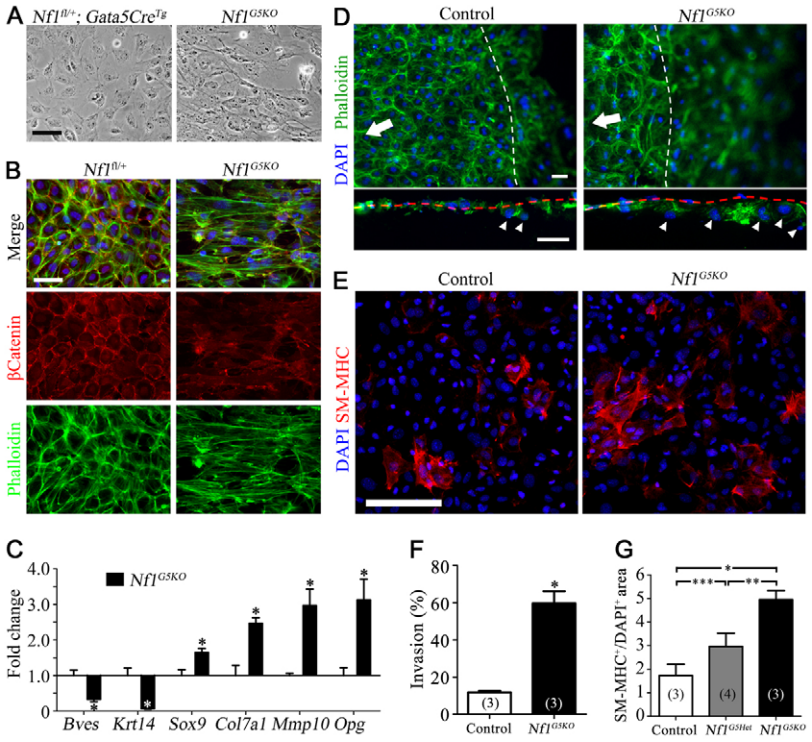

Fig. 2. Loss of Nf1 in epicardial cells results in a phenotypic change to mesenchymal cells in vitro. (**A**,**B**) Seventy-two hour primary cultured epicardial cells from E12.5 mouse hearts. (A) Brightfield images. (B) Cultures stained for adherens junctions (β-catenin) and actin stress fibers (phalloidin). Nuclei were detected with DAPI. (**C**) mRNA expression of epithelial (*Bves*, *Krt14*) and mesenchymal (*Sox9*, *Col7a1*, *Mmp10*, *Opg*) genes. qRT-PCR was used to quantify gene expression in primary epicardial cell cultures. Data were compared with control cultures represented by a baseline of 1.0. For each gene, at least five independent experiments were quantified in triplicate. Values are mean ± s.d. *P<0.0001. (**D**) Embryonic hearts of the indicated genotype were cultured on collagen gels to measure invasion. Actin stress fibers were stained with phalloidin and nuclei were detected with DAPI. Arrows indicate the center of the heart explants and white dashed lines delineate the invasion front. Invasion of epicardial cells was detected by fluorescence microscopy after sectioning (bottom). Red dashed lines indicate the collagen gel surface and arrowheads indicate invading cells. (**E**) Differentiation of epicardial cells into smooth muscle cells was detected by IHC for SM-MHC. Actin and nuclei were visualized with phalloidin and DAPI, respectively. (**F**) Quantification of invasion of epicardial cells into the collagen gel. Values are mean ± s.d. *P<0.0001. (**G**) Quantification of VSMC differentiation. The SM-MHC fluorescent area was normalized to the nuclear area. Data are mean ± s.d. n values are indicated in parentheses. *P<0.001; **P<0.005; ***P<0.05. Scale bars: 50 μm in A,B,D; 100 μm in E.

filamentous actin, respectively. Control epicardial cells maintained cell-cell contacts, had extensive cellular junctions and exhibited cortical actin. However, *Nf1*^{G5KO} epicardial cells formed extensive actin stress fibers and lost their junctions (Fig. 2B). These changes were inhibited by the Rho-associated protein kinase inhibitor Y27632 (Uehata et al., 1997), suggesting that known EMT signaling pathways were occurring in the *Nf1* mutant cultures (data not shown). These results also demonstrated a cell-autonomous role for Nf1 in regulating EMT.

Although morphology is commonly used as a readout for EMT, changes in gene expression profiles from epithelial to mesenchymal can also be used to detect the transition. We measured the expression of epithelial markers, such as *Krt14* (Chamulitrat et al., 2003; Ke et al., 2008) and *Bves* (Wada et al., 2001), by qRT-PCR (Fig. 2C). Consistent with a switch from epithelial to mesenchymal cell type, we found that epithelial gene expression was downregulated in *Nf1*^{G5KO} cultures. By contrast, mesenchymal gene expression, as indicated by *Col7a1* (Vindevoghel et al., 1998), *Mmp10* (Wilkins-Port and Higgins, 2007), *Sox9* (Cheung et al., 2005; Sakai et al., 2006) and *Opg* (*Tnfrsf11b* – Mouse Genome Informatics) (Corallini et al., 2009; Sakata et al., 1999; Vidal et al., 1998), was upregulated (Fig. 2C). We also observed an increased level of mesenchymal gene expression in heterozygous cultures (data not shown).

An additional criterion for transition from an epithelial to a mesenchymal phenotype is invasion into a collagen gel (Thiery and Sleeman, 2006). In a collagen gel assay (Boyer et al., 1999; Potts et al., 1991), ~12% of control epicardial cells invaded the collagen gel along the edge of the culture (Fig. 2D,F). In *Nf1*^{G5KO} epicardial cultures, ~60% of the cells in the same perimeter of the epicardial culture invaded the collagen gel and formed actin stress fibers (Fig. 2D,F).

When epicardial cells undergo EMT they differentiate predominantly into two cell types: cVSMCs and cardiac fibroblasts (Mikawa and Gourdie, 1996; Vrancken Peeters et al., 1999). To determine whether the increased EMT led to an increase in differentiated cells in vitro, we examined the expression of SM-MHC, a smooth muscle cell marker. Epicardial cultures from *Nf1*^{G5KO} and to a lesser extent *Nf1* heterozygous hearts exhibited an increased number of SM-MHC-expressing cells compared with control cultures (Fig. 2E,G).

In summary, *Nf1* mutant epicardial cells spontaneously lost epithelial characteristics and adopted a mesenchymal phenotype, including an increase in mesenchymal gene expression, invasiveness and differentiation. It should be noted that loss of Nf1 resulted in EMT under basal culture conditions. Therefore, these cultured epicardial cells might be poised to undergo EMT, and signaling by Nf1 could be a key regulatory pathway inhibiting this process.

Loss of Nf1 enhances EMT of epicardial cells in vivo

To determine whether the loss of Nf1 has a direct effect on EMT, we induced temporal deletions of *Nf1* between stages E10.5 and E12.5. These embryos therefore had wild-type expression of Nf1 until just before the stage of EMT. This tracing resulted in efficient R26R^{T} reporter expression in a high percentage of the epicardium (Fig. 3A). We then quantified the number of EPDCs that had migrated into the heart ventricle using whole-mount confocal microscopy at each time point. Fig. 3 is representative of optical sections comparing control and *Nf1*^{WTiKO} hearts (see supplementary material Fig. S3 for images at other time points). At E11.5, very few R26R^{T}-positive cells were detected in the control myocardial compartment (Fig. 3A,B; supplementary material Fig. S3). Tagged epicardial cells were observed in the ventricle at E12.5 and further increased at E13.5, suggesting that EMT began at ~E12.5 in control hearts (Fig. 3B; supplementary material Fig. S3). However, in *Nf1*^{WTiKO} hearts, at each time point examined a greater number of R26R^{T}-positive cells was detected within the myocardial compartment (Fig. 3A,B; supplementary material Fig. S3). The

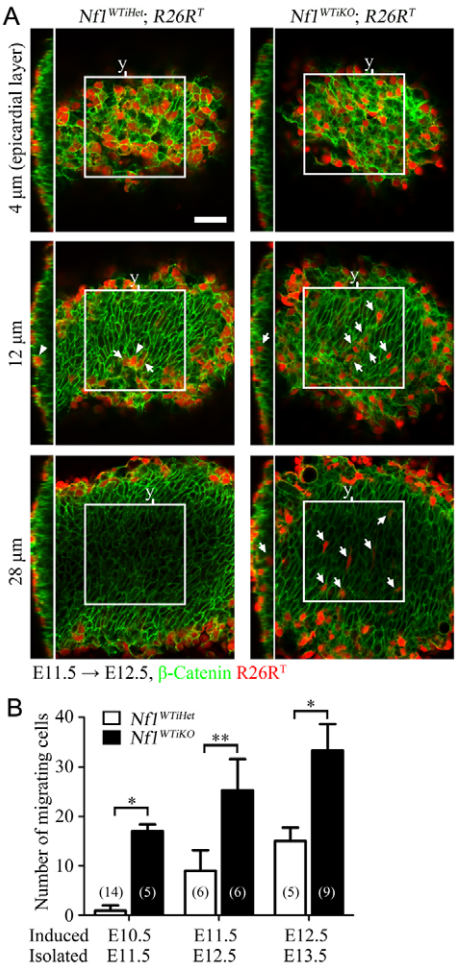

Fig. 3. Early and increased EMT in vivo upon the loss of Nf1 in epicardial cells. (**A**) Representative whole-mount confocal optical sections of the indicated genotype. Induction by tamoxifen was at E11.5, hearts were isolated at E12.5 and whole-mount-stained for β-catenin to distinguish individual cells. *z*-stack images were taken from the epicardium (defined as 0 μm) using a confocal microscope. Nine consecutive images of 4 μm optical thickness spanning a total of 32 μm were taken in similar regions of the heart left ventricle. Examples at 4, 12 and 28 μm depth are shown. Boxed regions indicate the area used for quantification (150 μm × 150 μm). An orthogonal view of the indicated *y*-axis (*y*) of each *z*-stacked image is shown to the left. Arrows indicate examples of migrated cells in the heart ventricular region. Arrowheads indicate cells in the epicardium. See supplementary material Fig. S3 for examples of the full panel of images at each tracing time point. Scale bar: 50 μm. (**B**) Quantification of R26R^{T}-positive cells in the myocardial region of hearts at the indicated tracing time points. The number of R26R^{T}-positive cells in the left ventricular region of the myocardial area (150 μm × 150 μm × 32 μm) was counted using ImageJ. Data are mean ± s.d. *n* values are indicated in parentheses. *P<0.0001; **P<0.0005.

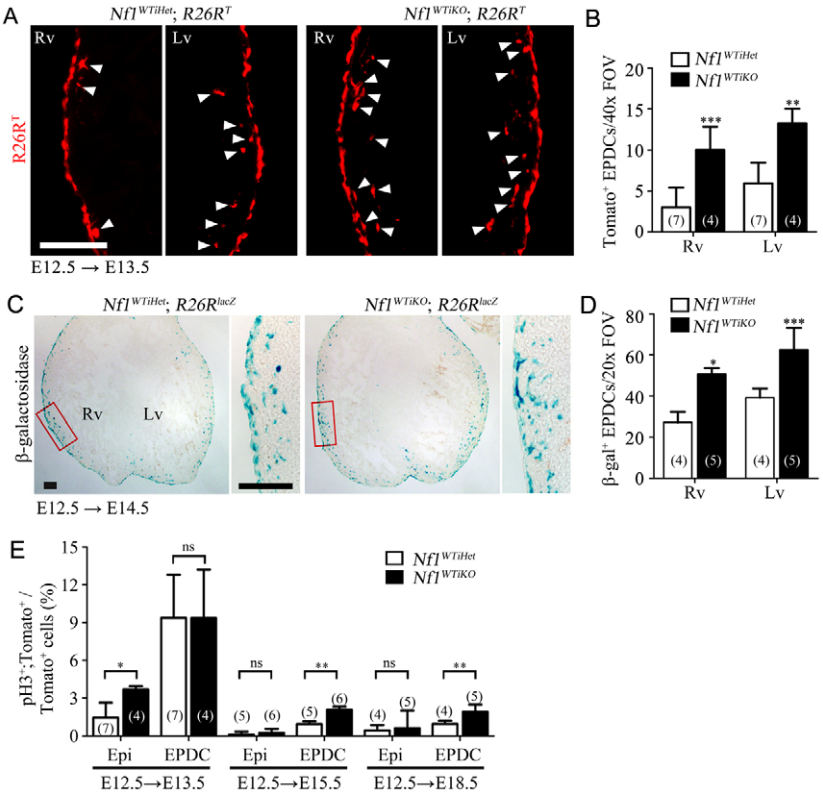

Fig. 4. Migration and proliferation of EPDCs after inactivation of *Nf1* in vivo. (**A**,**C**) R26R^{T} (A) and R26R^{lacZ} (C) epicardial lineage tracing was used to identify migrated epicardial cells in hearts of the indicated genotype. Induction with tamoxifen was at E12.5, and heart sections were imaged for R26R^{T} fluorescence at E13.5 (A) or stained for β-galactosidase activity at E14.5 (C). In C, the boxed regions are shown at higher magnification in the insets. Arrowheads in A designate EPDCs expressing R26R^{T}. Scale bars: 100 μm. (**B**,**D**) Quantification of migrated R26R^{T}-positive or R26R^{lacZ}-positive EPDCs in A and C, respectively. Images were taken from similar regions of heart in both left and right ventricles with a 40× or 20× field of view and counted for R26R^{T}-positive or R26R^{lacZ}-positive cells within the myocardial ventricular wall. Data are mean ± s.d. *n* values are indicated in parentheses. **P*<0.0001; ***P*<0.001; ****P*<0.005. (**E**) Quantification of Wt1 lineage-tagged cellular proliferation. Embryos were maternally induced with tamoxifen at E12.5. Heart sections were immunostained for phospho-histone H3 (pH3) to detect mitotic cells. The pH3^{+} Tomato^{+} cells were counted in epicardial or myocardial regions and normalized to the total number of Tomato^{+} cells in epicardium (Epi) or myocardial ventricular wall (EPDC). Nuclei were visualized with DAPI for quantification and images were taken from similar regions of heart in both left and right ventricles with a 20× field of view. *n* values are indicated in parentheses. **P*<0.01; ***P*<0.05; ns, no significant difference. Rv, right ventricle; Lv, left ventricle; FOV, field of view.

existence of migrated mutant epicardial cells at E11.5 suggested that epicardial EMT occurs earlier in the mutant hearts, and the increase in migrated epicardial cells demonstrated that, as in vitro, loss of Nf1 results in an increased number of cells undergoing EMT. Because confocal imaging only allowed us to examine a small region and time window of migrated epicardial cells, we also traced EPDCs in heart sections using two different reporters. A similar increase in R26R^{T}-positive or R26R^{lacZ}-positive EPDCs was detected at E13.5 and E14.5, respectively, upon loss of Nf1 at E12.5 in both the right and left ventricle (Fig. 4A-D).

To determine how loss of Nf1 impacted the proliferation and survival of epicardial cells and EPDCs at later stages of development, we inactivated Nf1 at E12.5 and quantified the number of proliferating (phospho-histone H3^{+}) cells within the R26R^{T}-positive epicardial and EPDC population. At E13.5 we saw a modest increase in proliferation of Nf1-deficient epicardial cells (Fig. 4E). At the same stage, a similar number of the EPDCs in both control and mutant hearts were in mitosis (Fig. 4E). However, at later stages, Nf1-deficient EPDCs exhibited increased proliferation (Fig. 4E). Because alterations in cell survival have been reported in Nf1-deficient endocardial cushions (Lakkis and Epstein, 1998), we examined *Nf1^{WTiKO}* and *Nf1^{G5KO}* hearts for apoptosis, using an antibody for cleaved caspase 3, at various time points from E12.5 to P0. No differences in apoptotic cell numbers were observed between control and mutant hearts (data not shown).

Epicardial inactivation of *Nf1* results in expansion of cardiac fibroblasts and cVSMCs in vivo

Because enhanced epicardial cell EMT and EPDC proliferation were observed, we reasoned that there might be an expansion of EPDCs. As cardiac fibroblasts and cVSMCs are the predominant populations of cells derived from the epicardium, we determined how loss of Nf1 impacted these cells. Using in situ hybridization for three genes that identify cardiac fibroblasts, namely *Col1a1*, *Col3a1* and *Pdgfra* (Smith et al., 2011), we found an increased number of cardiac fibroblasts in mutant hearts compared with controls (Fig. 5A,C). Collagen I is also expressed by some VSMCs (Ponticos et al., 2004) and therefore it is likely that this particular probe overestimated the number of fibroblasts, but the data clearly demonstrated an increase in non-vessel-associated *Col1a1*-expressing, as well as *Col3a1*- and *Pdgfra*-expressing, cells. This increase in cell numbers was not restricted to the cardiac fibroblast lineage. We utilized the *X-LacZ4^{Tg}* mouse (Tidhar et al., 2001) that expresses a nuclear-localized β-galactosidase in VSMCs and efficiently tags cVSMCs (Mellgren et al., 2008). We found that loss of Nf1 also resulted in an expansion of the VSMC lineage (Fig. 5B). Not only were more cVSMCs detected at E17.5, but the increase also appeared to lead to an extended and more highly branched cVSMC-coated network of coronary vasculature (Fig. 5D; data not shown).

Nf1 regulation of Ras signaling plays a role in PDGF-induced epicardial EMT

It is established that loss of Nf1 leads to prolonged activation of the Ras-MAPK pathway in cardiomyocytes and VSMCs (Cichowski and Jacks, 2001; Xu et al., 2009a; Xu et al., 2007). To determine whether activation of Erk1/2 (Mapk3/1 – Mouse Genome Informatics) is responsible for EMT in Nf1-deficient epicardial cells, we inhibited the MAP kinase pathway and measured EMT by ex vivo migration assay (Mellgren et al., 2008). The epicardium of E12.5 hearts was labeled by adenoviral GFP transduction, and migration of GFP-expressing epicardial cells into the myocardium was quantified. In control hearts, GFP^{+} cells were restricted to the epicardium, whereas *Nf1^{G5KO}* hearts possessed an increased

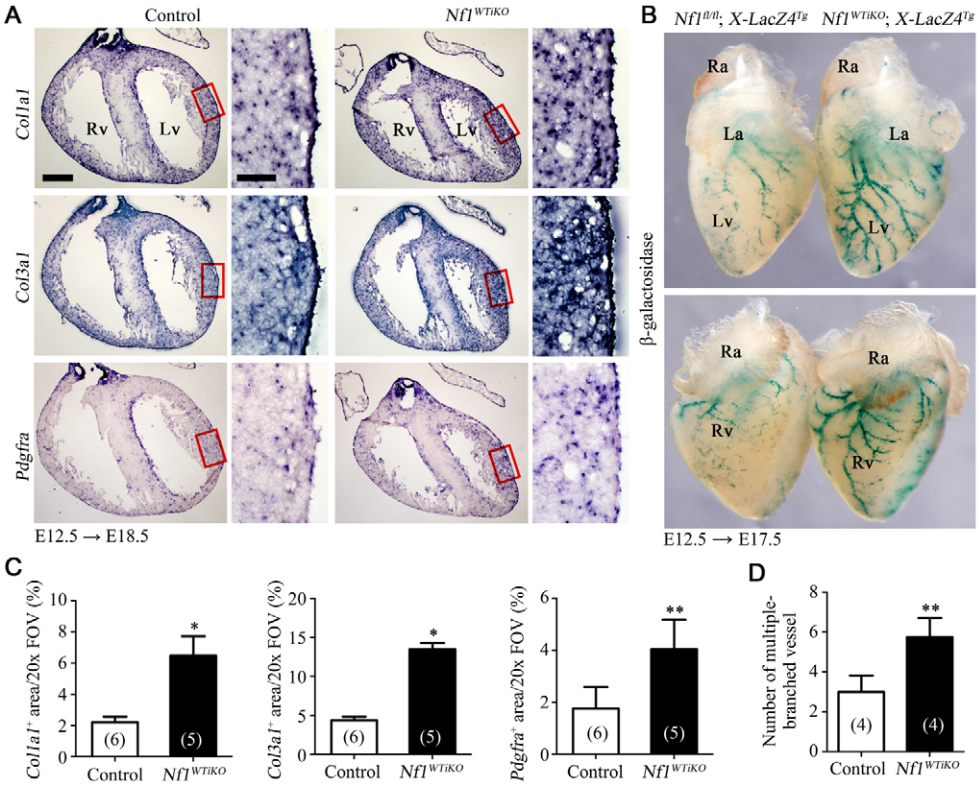

Fig. 5. Expansion of EPDCs upon loss of Nf1 in the epicardium. (**A**) In situ hybridization at E18.5 for cardiac fibroblast marker genes (*Col1a1*, *Col3a1* and *Pdgfra*). Mouse embryos were induced with tamoxifen at E12.5 and hearts were isolated at E18.5. The boxed regions are shown at higher magnification in the insets. Scale bars: 500 μm; 100 μm in insets. (**B**) Whole-mount β-galactosidase staining (blue) of *X-LacZ4* hearts for detection of VSMCs. Tamoxifen was administrated maternally at E12.5 before heart isolation at E17.5. (**C**) Quantification of the area positive for *Col1a1*, *Col3a1* or *Pdgfra* in A from 20× field-of-view images taken in similar regions of the left ventricle. (**D**) Quantification of multi-branched (three or more) SMC-coated vessels in B. Data are mean ± s.d. *n* values are indicated in parentheses. **P*<0.001; ***P*<0.005. Ra, right atrium; La, left atrium; Rv, right ventricle; Lv, left ventricle; FOV, field of view.

number of GFP$^+$ cells within the myocardium, suggesting an enhanced ability of *Nf1*-null epicardial cells to leave the epicardial layer (Fig. 6A,B). The increased migration was abolished when hearts were cultured in the presence of U0126, an inhibitor of both Mek1 and Mek2 (Map2k1 and Map2k2 – Mouse Genome Informatics) (Fig. 6A,B). These data suggest that activation of ERK is responsible for EMT in Nf1-deficient epicardial cells.

Loss of Nf1 alone does not lead to extended activation of Ras. Upstream signals are required to initiate Ras signaling, then in the absence of Nf1, Ras remains in its active state (McCormick, 1995). We have recently reported that PDGF receptor signaling is an essential component of epicardial EMT. Pdgfrα and Pdgfrβ are expressed in the epicardium, and inactivation of these receptors in epicardial cells disrupts EMT (Mellgren et al., 2008; Smith et al., 2011). To determine whether PDGF signaling could be one pathway upstream of Ras-Nf1 signaling, we inhibited PDGF receptor tyrosine kinase activity in *Nf1*^{G5KO} epicardial cells. Imatinib mesylate, a potent inhibitor of both Pdgfrα and Pdgfrβ, inhibited the EMT phenotype caused by loss of Nf1 in the epicardial culture EMT assay (data not shown) and the ex vivo migration of epicardial cells (Fig. 6A,B). Similar results were obtained using AG1296, another inhibitor of the PDGF receptors (data not shown).

Next, we tested whether Nf1 Ras-GAP activity could negatively regulate PDGF-induced EMT in the ex vivo migration assay. Stimulation with recombinant PDGF-BB induced epicardial cell migration into the myocardium; however, adenoviral transduction of the Nf1 GAP-related domain (Nf1-GRD) (Hiatt et al., 2001; Miller et al., 2010) significantly reduced PDGF-BB-induced EMT (Fig. 6C,D). Conversely, we determined whether activation of Ras induced epicardial EMT using epicardial cultures from *K-Ras(G12D)*$^{fl/+}$ embryos. This transgene expresses a Cre-inducible oncogenic form of Kras (Jackson et al., 2001). Whereas control cultures had intact cellular junctions with cortical actin, when *K-Ras(G12D)* expression was induced the epicardial cultures formed actin stress fibers and lost cellular junctions, similar to *Nf1*$^{fl/fl}$ cultures (Fig. 6E). Similarly, *K-Ras*$^{fl/+}$*;Wt1*$^{CreERT2/+}$ hearts had an increased number of Wt1$^+$ cells in the myocardial compartment. This suggests that activation of Ras also results in increased epicardial EMT in vivo (Fig. 6F,G).

Finally, we determined whether loss of Pdgfrα signaling could partially rescue the excess EMT observed in the *Nf1*^{WTiKO} heart. As loss of Pdgfrα specifically affects only cardiac fibroblast progenitor EMT (Smith et al., 2011), we predicted that loss of Pdgfrα in an *Nf1*^{WTiKO} mutant background would lead to a reduction in EPDCs entering the epicardium as compared with an *Nf1*^{WTiKO} mutant that possessed Pdgfrα signaling. Consistent with our previous data, *Nf1*^{WTiKO} hearts had more Wt1$^+$ cells within the myocardium than wild-type controls; however, simultaneous inactivation of both *Pdgfra* and *Nf1* resulted in a significant reduction of migrated Wt1$^+$ cells (Fig. 6F,G). One reason for the partial rescue of the *Nf1*^{WTiKO} EMT phenotype could be the presence of VSMC progenitors, which still express Pdgfrβ (Mellgren et al., 2008; Smith et al., 2011) and should continue to have excess Ras signaling due to loss of Nf1.

In conclusion, our results show that Nf1 is a key regulator of epicardial EMT and that this increased EMT as well as an increased rate of proliferation result in expansion of cardiac fibroblasts and VSMCs.

DISCUSSION

EMT is an essential process that plays a significant role in embryogenesis during gastrulation, heart development and neural crest cell formation (Thiery et al., 2009). There is now very compelling evidence that EMT is an essential component of tumor metastasis (Thiery et al., 2009; Yang and Weinberg, 2008). Because

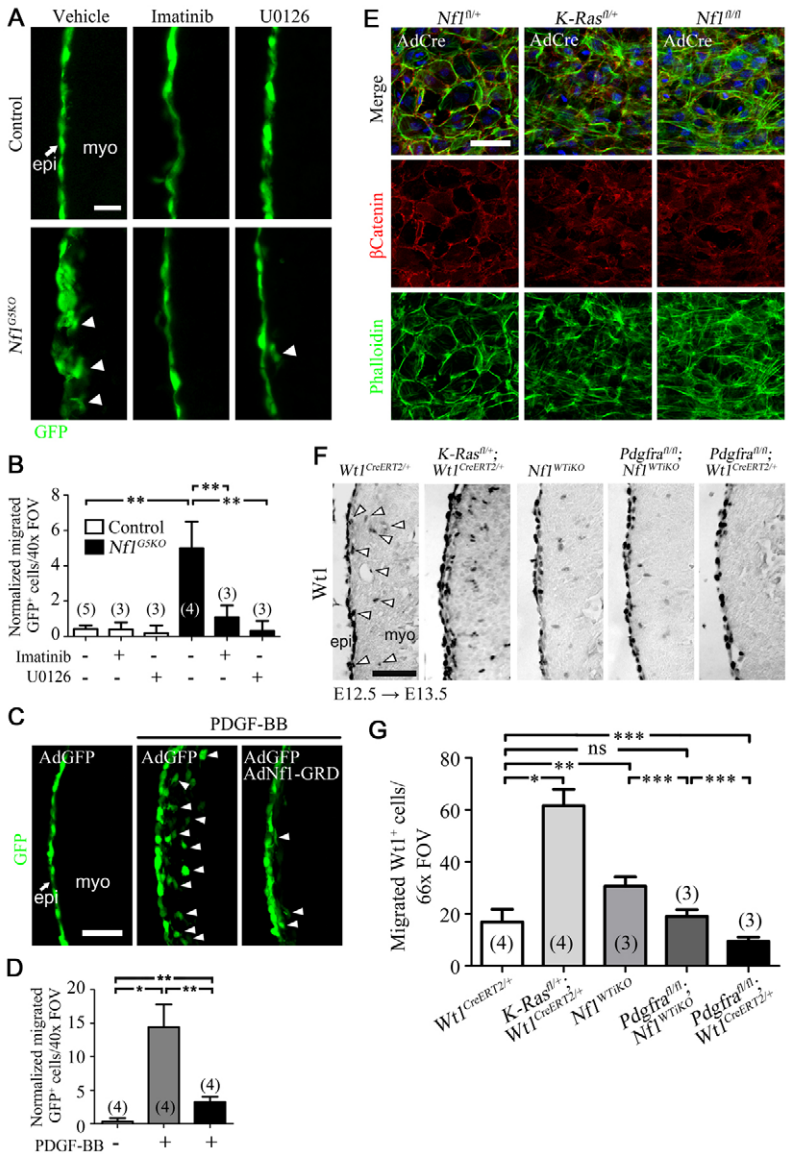

Fig. 6. Regulation of epicardial EMT by Nf1. (**A**,**C**) Representative GFP fluorescence images of the ex vivo migration assay. E12.5 mouse hearts were cultured and epicardial cells were labeled by adenoviral GFP transduction. Arrowheads indicate epicardial cell migration. Arrow indicates epicardium (epi); myo, myocardium. (A) Hearts were treated with 2 μM imatinib mesylate (a potent inhibitor of both Pdgfrα and Pdgfrβ) or U0126 (an inhibitor of both Mek1 and Mek2) where indicated. Hearts were cultured for 2 days before analyzing migration by GFP fluorescence. (C) Hearts were cultured in the presence or absence of Nf1 GAP-related domain (Nf1-GRD) adenovirus. After 18 hours, recombinant PDGF-BB was added to a final concentration of 20 ng/ml. Hearts were then cultured for 2 more days before analyzing migration by GFP fluorescence. (**B**,**D**) Quantification of migration in A and C, respectively. Migrated GFP$^+$ cells were quantified and normalized by multiplying by adenoviral transduction efficiency (GFP$^+$ cells in epicardium/total number of epicardial cells in a 40× field of view). Data are mean ± s.d. *n* values are indicated in parentheses. **P*<0.0005; ***P*<0.001. (**E**) Representative fluorescent images of primary epicardial cell cultures. E12.5 hearts of the indicated genotype were isolated and cultured on collagen-coated coverslips for 3 days. Heart explants were then removed and adenovirus for Cre expression (AdCre) added to the cultures. After 2 days, cells were fixed and stained with phalloidin and anti-β-catenin antibody to visualize actin stress fibers and cellular junctions, respectively. Nuclei were detected with DAPI. (**F**) IHC for Wt1 in left ventricle of the indicated genotype. Images were taken in a 66× field of view and Wt1$^+$ cells in the subepicardium and ventricle were quantified. Arrowheads illustrate cells that would be quantified. Cropped images of quantified regions are shown. Induction by tamoxifen was at E12.5 and hearts were isolated after 24 hours. (**G**) Quantification of Wt1$^+$ cells in F. Wt1$^+$ cells in the myocardial compartment of the left ventricle were counted in 66× field-of-view images. Data are mean ± s.d. *n* values are indicated in parentheses. **P*<0.0001; ***P*<0.001; ****P*<0.05; ns, no significant difference. FOV, field of view. Scale bars: 200 μm in A; 50 μm in C,E,F.

the best-known activity for Nf1 is its GAP activity, it is assumed that loss of Nf1 leads to abnormal Ras signaling. A further link with EMT can then be drawn because Ras signaling can induce EMT. One mechanism is by cooperating with TGFβ to promote Snail transcriptional activity (Horiguchi et al., 2009; Janda et al., 2002). Another is by activating MAPK and Rac, potentially leading to disruption of epithelial junctions (Edme et al., 2002). In fact, many of the EMT-inducing abilities of epidermal growth factor and hepatocyte growth factor have been directly linked to Ras activity (Boyer et al., 1997; Herrera, 1998). Here, we provide evidence that loss of *Nf1* increases EMT in mouse epicardial cells, suggesting a possible regulatory role for Nf1 in Ras-driven EMT.

Interestingly, loss of Nf1 does not lead to persistent EMT. Instead, the EMT we observed is only amplified by occurring earlier and more robustly, as might be expected by its downstream signaling role. Nf1 does not initiate signaling (McCormick, 1995). Other factors must lie upstream to activate the Ras-MAPK pathway. Epicardial EMT is distinct from neural crest cell EMT in that only a subset of cells becomes mesenchymal, suggesting that the inductive signal is regionally localized and controlled temporally, thus providing an explanation for why epicardial EMT in the absence of Nf1 is still partially restricted. Indeed, we have shown that by inhibiting one of these potential upstream growth factor pathways, i.e. PDGF (Mellgren et al., 2008; Smith et al., 2011), we can block the effects of loss of Nf1. Interestingly, increased neointima formation in *Nf1* heterozygous mice can also be mitigated by imatinib treatment, suggesting a possible role for PDGF signaling in the exaggerated vascular injury response that occurs upon the loss of *Nf1* (Lasater et al., 2008). Because inhibition of MAPK also blunted the effect of loss of Nf1 on EMT, it is likely that Nf1 attenuates these inductive signals only in the epicardial cells that have been stimulated to undergo EMT.

Cardiovascular disease is a frequent cause of death in patients with neurofibromatosis 1 who are less than 30 years old (Rasmussen et al., 2001). Although some of this lethality is attributed to congenital abnormalities (Friedman et al., 2002; Lin et al., 2000), our findings also point to the possibility that an increase in the proliferation of epicardial-derived noncardiomyocyte lineages might also contribute to some of the heart abnormalities. Loss of Nf1 did not lead to excessive overgrowth of these cells under normal circumstances. It is likely that local environmental cues ultimately determine the differentiation and survival of EPDCs. For example, endothelial cells, which secrete PDGF ligands, are important regulators of

cVSMC migration and proliferation (Tomanek, 2005). Similarly, local limitations of growth factor production by these cells might account for the lack of excessive cVSMC proliferation. Therefore, loss of Nf1 results in a controlled expansion of EPDCs rather than massive hyperplasia. This phenomenon would be reminiscent of what occurs with Nf1-mediated tumorigenicity, in which disruptions in the microenvironment are necessary for tumor progression (Zhu et al., 2002). Nonetheless, because loss of Nf1 is often linked to increased proliferation (Lynch and Gutmann, 2002) during a pathological response to heart injury, Nf1-deficient cells might respond more robustly by enhanced proliferation and fibrotic activity. Most neurofibromatosis 1 patients would be haploinsufficient in somatic cells, but our data and those of others suggest that even cells with reduced Nf1 protein might have elevated levels of GTP-bound Ras, thus leading to increased signaling and downstream cellular events (Atit et al., 1999; Ingram et al., 2000).

In summary, we demonstrate that epicardial loss of *Nf1* results in early and increased EMT, which leads to the expansion of cardiac fibroblasts and cVSMCs. We were able to mitigate the increased EMT by altering PDGF signaling, which has recently been implicated in epicardial EMT (Smith et al., 2011). Our work indicates that EPDCs, along with endocardial-derived valve cells and cardiomyocytes are sensitive to perturbations in Nf1 activity. Further investigations will be required to determine what the long-term outcomes of this EPDC expansion are for the physiology of the heart under pathological and non-pathological conditions.

Acknowledgements
We thank Ray Runyan for essential comments and help with the collagen gel invasion assay; Moshe Shani for providing the *X-LacZ4*^{Tg} mouse line; Nancy Ratner for providing Nf1-GRD adenovirus; Christopher Smith and other M.D.T. laboratory members for scientific discussion and critical reading of the manuscript; and Greg Urquhart, Banu Eskiocak and Emily Webster for technical assistance.

Funding
This work was supported by National Heart, Lung, and Blood Institute (NHLBI) grants from the National Institutes of Health [HL074257 and HL100401 to M.D.T.]; and an American Heart Association Predoctoral Fellowship [10PRE3730051 to S.T.B.]. Deposited in PMC for release after 12 months.

Competing interests statement
The authors declare no competing financial interests.

Supplementary material
Supplementary material available online at
http://dev.biologists.org/lookup/suppl/doi:10.1242/dev.074054/-/DC1

References

Acharya, A., Baek, S. T., Banfi, S., Eskiocak, B. and Tallquist, M. D. (2011). Efficient inducible Cre-mediated recombination in Tcf21cell lineages in the heart and kidney. *Genesis* **49**, 870-877.
Aoki, Y., Niihori, T., Kawame, H., Kurosawa, K., Ohashi, H., Tanaka, Y., Filocamo, M., Kato, K., Suzuki, Y., Kure, S. et al. (2005). Germline mutations in HRAS proto-oncogene cause Costello syndrome. *Nat. Genet.* **37**, 1038-1040.
Atit, R. P., Crowe, M. J., Greenhalgh, D. G., Wenstrup, R. J. and Ratner, N. (1999). The Nf1 tumor suppressor regulates mouse skin wound healing, fibroblast proliferation, and collagen deposited by fibroblasts. *J. Invest. Dermatol.* **112**, 835-842.
Bostrom, H., Willetts, K., Pekny, M., Leveen, P., Lindahl, P., Hedstrand, H., Pekna, M., Hellstrom, M., Gebre-Medhin, S., Schalling, M. et al. (1996). PDGF-A signaling is a critical event in lung alveolar myofibroblast development and alveogenesis. *Cell* **85**, 863-873.
Boyer, A. S., Ayerinskas, I. I., Vincent, E. B., McKinney, L. A., Weeks, D. L. and Runyan, R. B. (1999). TGFbeta2 and TGFbeta3 have separate and sequential activities during epithelial-mesenchymal cell transformation in the embryonic heart. *Dev. Biol.* **208**, 530-545.
Boyer, B., Roche, S., Denoyelle, M. and Thiery, J. P. (1997). Src and Ras are involved in separate pathways in epithelial cell scattering. *EMBO J.* **16**, 5904-5913.
Brannan, C. I., Perkins, A. S., Vogel, K. S., Ratner, N., Nordlund, M. L., Reid, S. W., Buchberg, A. M., Jenkins, N. A., Parada, L. F. and Copeland, N. G. (1994). Targeted disruption of the neurofibromatosis type-1 gene leads to developmental abnormalities in heart and various neural crest-derived tissues. *Genes Dev.* **8**, 1019-1029.
Chamulitrat, W., Schmidt, R., Chunglok, W., Kohl, A. and Tomakidi, P. (2003). Epithelium and fibroblast-like phenotypes derived from HPV16 E6/E7-immortalized human gingival keratinocytes following chronic ethanol treatment. *Eur. J. Cell Biol.* **82**, 313-322.
Cheung, M., Chaboissier, M. C., Mynett, A., Hirst, E., Schedl, A. and Briscoe, J. (2005). The transcriptional control of trunk neural crest induction, survival, and delamination. *Dev. Cell* **8**, 179-192.
Cichowski, K. and Jacks, T. (2001). NF1 tumor suppressor gene function: narrowing the GAP. *Cell* **104**, 593-604.
Corallini, F., Gonelli, A., D'Aurizio, F., di Iasio, M. G. and Vaccarezza, M. (2009). Mesenchymal stem cells-derived vascular smooth muscle cells release abundant levels of osteoprotegerin. *Eur. J. Histochem.* **53**, 19-24.
de Lange, F. J., Moorman, A. F., Anderson, R. H., Manner, J., Soufan, A. T., de Gier-de Vries, C., Schneider, M. D., Webb, S., van den Hoff, M. J. and Christoffels, V. M. (2004). Lineage and morphogenetic analysis of the cardiac valves. *Circ. Res.* **95**, 645-654.
Dettman, R. W., Denetclaw, W., Jr, Ordahl, C. P. and Bristow, J. (1998). Common epicardial origin of coronary vascular smooth muscle, perivascular fibroblasts, and intermyocardial fibroblasts in the avian heart. *Dev. Biol.* **193**, 169-181.
Edme, N., Downward, J., Thiery, J. P. and Boyer, B. (2002). Ras induces NBT-II epithelial cell scattering through the coordinate activities of Rac and MAPK pathways. *J. Cell Sci.* **115**, 2591-2601.
Friedman, J. M., Arbiser, J., Epstein, J. A., Gutmann, D. H., Huot, S. J., Lin, A. E., McManus, B. and Korf, B. R. (2002). Cardiovascular disease in neurofibromatosis 1, report of the NF1 Cardiovascular Task Force. *Genet. Med.* **4**, 105-111.
Gitler, A. D., Zhu, Y., Ismat, F. A., Lu, M. M., Yamauchi, Y., Parada, L. F. and Epstein, J. A. (2003). Nf1 has an essential role in endothelial cells. *Nat. Genet.* **33**, 75-79.
Hamilton, T. G., Klinghoffer, R. A., Corrin, P. D. and Soriano, P. (2003). Evolutionary divergence of platelet-derived growth factor alpha receptor signaling mechanisms. *Mol. Cell. Biol.* **23**, 4013-4025.
Herrera, R. (1998). Modulation of hepatocyte growth factor-induced scattering of HT29 colon carcinoma cells. Involvement of the MAPK pathway. *J. Cell Sci.* **111**, 1039-1049.
Hiatt, K. K., Ingram, D. A., Zhang, Y., Bollag, G. and Clapp, D. W. (2001). Neurofibromin GTPase-activating protein-related domains restore normal growth in Nf1–/– cells. *J. Biol. Chem.* **276**, 7240-7245.
Horiguchi, K., Shirakihara, T., Nakano, A., Imamura, T., Miyazono, K. and Saitoh, M. (2009). Role of Ras signaling in the induction of snail by transforming growth factor-beta. *J. Biol. Chem.* **284**, 245-253.
Ingram, D. A., Yang, F. C., Travers, J. B., Wenning, M. J., Hiatt, K., New, S., Hood, A., Shannon, K., Williams, D. A. and Clapp, D. W. (2000). Genetic and biochemical evidence that haploinsufficiency of the Nf1 tumor suppressor gene modulates melanocyte and mast cell fates in vivo. *J. Exp. Med.* **191**, 181-188.
Jacks, T., Shih, T. S., Schmitt, E. M., Bronson, R. T., Bernards, A. and Weinberg, R. A. (1994). Tumour predisposition in mice heterozygous for a targeted mutation in Nf1. *Nat. Genet.* **7**, 353-361.
Jackson, E. L., Willis, N., Mercer, K., Bronson, R. T., Crowley, D., Montoya, R., Jacks, T. and Tuveson, D. A. (2001). Analysis of lung tumor initiation and progression using conditional expression of oncogenic K-ras. *Genes Dev.* **15**, 3243-3248.
Janda, E., Lehmann, K., Killisch, I., Jechlinger, M., Herzig, M., Downward, J., Beug, H. and Grunert, S. (2002). Ras and TGF[beta] cooperatively regulate epithelial cell plasticity and metastasis: dissection of Ras signaling pathways. *J. Cell Biol.* **156**, 299-313.
Ke, X. S., Qu, Y., Goldfinger, N., Rostad, K., Hovland, R., Akslen, L. A., Rotter, V., Oyan, A. M. and Kalland, K. H. (2008). Epithelial to mesenchymal transition of a primary prostate cell line with switches of cell adhesion modules but without malignant transformation. *PLoS ONE* **3**, e3368.
Kontaridis, M. I., Swanson, K. D., David, F. S., Barford, D. and Neel, B. G. (2006). PTPN11 (Shp2) mutations in LEOPARD syndrome have dominant negative, not activating, effects. *J. Biol. Chem.* **281**, 6785-6792.
Lakkis, M. M. and Epstein, J. A. (1998). Neurofibromin modulation of ras activity is required for normal endocardial-mesenchymal transformation in the developing heart. *Development* **125**, 4359-4367.
Lasater, E. A., Bessler, W. K., Mead, L. E., Horn, W. E., Clapp, D. W., Conway, S. J., Ingram, D. A. and Li, F. (2008). Nf1+/– mice have increased neointima formation via hyperactivation of a Gleevec sensitive molecular pathway. *Hum. Mol. Genet.* **17**, 2336-2344.
Lie-Venema, H., van den Akker, N. M., Bax, N. A., Winter, E. M., Maas, S., Kekarainen, T., Hoeben, R. C., deRuiter, M. C., Poelmann, R. E. and Gittenberger-de Groot, A. C. (2007). Origin, fate, and function of epicardium-

derived cells (EPDCs) in normal and abnormal cardiac development. *ScientificWorldJournal* **7**, 1777-1798.
Lin, A. E., Birch, P. H., Korf, B. R., Tenconi, R., Niimura, M., Poyhonen, M., Armfield Uhas, K., Sigorini, M., Virdis, R., Romano, C. et al. (2000). Cardiovascular malformations and other cardiovascular abnormalities in neurofibromatosis 1. *Am. J. Med. Genet.* **95**, 108-117.
Lu, J., Richardson, J. A. and Olson, E. N. (1998). Capsulin: a novel bHLH transcription factor expressed in epicardial progenitors and mesenchyme of visceral organs. *Mech. Dev.* **73**, 23-32.
Lynch, T. M. and Gutmann, D. H. (2002). Neurofibromatosis 1. *Neurol. Clin.* **20**, 841-865.
Madisen, L., Zwingman, T. A., Sunkin, S. M., Oh, S. W., Zariwala, H. A., Gu, H., Ng, L. L., Palmiter, R. D., Hawrylycz, M. J., Jones, A. R. et al. (2010). A robust and high-throughput Cre reporting and characterization system for the whole mouse brain. *Nat. Neurosci.* **13**, 133-140.
Manner, J., Perez-Pomares, J. M., Macias, D. and Munoz-Chapuli, R. (2001). The origin, formation and developmental significance of the epicardium: a review. *Cells Tissues Organs* **169**, 89-103.
Martin, G. A., Viskochil, D., Bollag, G., McCabe, P. C., Crosier, W. J., Haubruck, H., Conroy, L., Clark, R., O'Connell, P., Cawthon, R. M. et al. (1990). The GAP-related domain of the neurofibromatosis type 1 gene product interacts with ras p21. *Cell* **63**, 843-849.
McCormick, F. (1995). Ras signaling and NF1. *Curr. Opin. Genet. Dev.* **5**, 51-55.
Mellgren, A. M., Smith, C. L., Olsen, G. S., Eskiocak, B., Zhou, B., Kazi, M. N., Ruiz, F. R., Pu, W. T. and Tallquist, M. D. (2008). Platelet-derived growth factor receptor beta signaling is required for efficient epicardial cell migration and development of two distinct coronary vascular smooth muscle cell populations. *Circ. Res.* **103**, 1393-1401.
Mercado-Pimentel, M. E. and Runyan, R. B. (2007). Multiple transforming growth factor-beta isoforms and receptors function during epithelial-mesenchymal cell transformation in the embryonic heart. *Cells Tissues Organs* **185**, 146-156.
Merki, E., Zamora, M., Raya, A., Kawakami, Y., Wang, J., Zhang, X., Burch, J., Kubalak, S. W., Kaliman, P., Belmonte, J. C. et al. (2005). Epicardial retinoid X receptor alpha is required for myocardial growth and coronary artery formation. *Proc. Natl. Acad. Sci. USA* **102**, 18455-18460.
Mikawa, T. and Gourdie, R. G. (1996). Pericardial mesoderm generates a population of coronary smooth muscle cells migrating into the heart along with ingrowth of the epicardial organ. *Dev. Biol.* **174**, 221-232.
Miller, S. J., Lan, Z. D., Hardiman, A., Wu, J., Kordich, J. J., Patmore, D. M., Hegde, R. S., Cripe, T. P., Cancelas, J. A., Collins, M. H. et al. (2010). Inhibition of Eyes Absent Homolog 4 expression induces malignant peripheral nerve sheath tumor necrosis. *Oncogene* **29**, 368-379.
Moore, A. W., McInnes, L., Kreidberg, J., Hastie, N. D. and Schedl, A. (1999). YAC complementation shows a requirement for Wt1 in the development of epicardium, adrenal gland and throughout nephrogenesis. *Development* **126**, 1845-1857.
Morgan, S. C., Lee, H. Y., Relaix, F., Sandell, L. L., Levorse, J. M. and Loeken, M. R. (2008). Cardiac outflow tract septation failure in Pax3-deficient embryos is due to p53-dependent regulation of migrating cardiac neural crest. *Mech. Dev.* **125**, 757-767.
Niihori, T., Aoki, Y., Narumi, Y., Neri, G., Cave, H., Verloes, A., Okamoto, N., Hennekam, R. C., Gillessen-Kaesbach, G., Wieczorek, D. et al. (2006). Germline KRAS and BRAF mutations in cardio-facio-cutaneous syndrome. *Nat. Genet.* **38**, 294-296.
Pennisi, D. J. and Mikawa, T. (2009). FGFR-1 is required by epicardium-derived cells for myocardial invasion and correct coronary vascular lineage differentiation. *Dev. Biol.* **328**, 148-159.
Perez-Pomares, J. M., Macias, D., Garcia-Garrido, L. and Munoz-Chapuli, R. (1997). Contribution of the primitive epicardium to the subepicardial mesenchyme in hamster and chick embryos. *Dev. Dyn.* **210**, 96-105.
Ponticos, M., Partridge, T., Black, C. M., Abraham, D. J. and Bou-Gharios, G. (2004). Regulation of collagen type I in vascular smooth muscle cells by competition between Nkx2.5 and deltaEF1/ZEB1. *Mol. Cell. Biol.* **24**, 6151-6161.
Potts, J. D., Dagle, J. M., Walder, J. A., Weeks, D. L. and Runyan, R. B. (1991). Epithelial-mesenchymal transformation of embryonic cardiac endothelial cells is inhibited by a modified antisense oligodeoxynucleotide to transforming growth factor beta 3. *Proc. Natl. Acad. Sci. USA* **88**, 1516-1520.
Rasmussen, S. A., Yang, Q. and Friedman, J. M. (2001). Mortality in neurofibromatosis 1, an analysis using U.S. death certificates. *Am. J. Hum. Genet.* **68**, 1110-1118.
Sakai, D., Suzuki, T., Osumi, N. and Wakamatsu, Y. (2006). Cooperative action of Sox9, Snail2 and PKA signaling in early neural crest development. *Development* **133**, 1323-1333.
Sakata, M., Shiba, H., Komatsuzawa, H., Fujita, T., Ohta, K., Sugai, M., Suginaka, H. and Kurihara, H. (1999). Expression of osteoprotegerin (osteoclastogenesis inhibitory factor) in cultures of human dental mesenchymal cells and epithelial cells. *J. Bone Miner. Res.* **14**, 1486-1492.
Schaeren-Wiemers, N. and Gerfin-Moser, A. (1993). A single protocol to detect transcripts of various types and expression levels in neural tissue and cultured cells: in situ hybridization using digoxigenin-labelled cRNA probes. *Histochemistry* **100**, 431-440.
Schubbert, S., Zenker, M., Rowe, S. L., Boll, S., Klein, C., Bollag, G., van der Burgt, I., Musante, L., Kalscheuer, V., Wehner, L. E. et al. (2006). Germline KRAS mutations cause Noonan syndrome. *Nat. Genet.* **38**, 331-336.
Smith, C. L., Baek, S. T., Sung, C. Y. and Tallquist, M. D. (2011). Epicardial-derived cell epithelial-to-mesenchymal transition and fate specification require PDGF receptor signaling. *Circ. Res.* **108**, e15-e26.
Soriano, P. (1999). Generalized lacZ expression with the ROSA26 Cre reporter strain. *Nat. Genet.* **21**, 70-71.
Sridurongrit, S., Larsson, J., Schwartz, R., Ruiz-Lozano, P. and Kaartinen, V. (2008). Signaling via the Tgf-beta type I receptor Alk5 in heart development. *Dev. Biol.* **322**, 208-218.
Tallquist, M. D., French, W. J. and Soriano, P. (2003). Additive effects of PDGF receptor beta signaling pathways in vascular smooth muscle cell development. *PLoS Biol.* **1**, E52.
Thiery, J. P. and Sleeman, J. P. (2006). Complex networks orchestrate epithelial-mesenchymal transitions. *Nat. Rev. Mol. Cell Biol.* **7**, 131-142.
Thiery, J. P., Acloque, H., Huang, R. Y. and Nieto, M. A. (2009). Epithelial-mesenchymal transitions in development and disease. *Cell* **139**, 871-890.
Tidhar, A., Reichenstein, M., Cohen, D., Faerman, A., Copeland, N. G., Gilbert, D. J., Jenkins, N. A. and Shani, M. (2001). A novel transgenic marker for migrating limb muscle precursors and for vascular smooth muscle cells. *Dev. Dyn.* **220**, 60-73.
Tomanek, R. J. (2005). Formation of the coronary vasculature during development. *Angiogenesis* **8**, 273-284.
Uehata, M., Ishizaki, T., Satoh, H., Ono, T., Kawahara, T., Morishita, T., Tamakawa, H., Yamagami, K., Inui, J., Maekawa, M. et al. (1997). Calcium sensitization of smooth muscle mediated by a Rho-associated protein kinase in hypertension. *Nature* **389**, 990-994.
Vidal, N. O., Brandstrom, H., Jonsson, K. B. and Ohlsson, C. (1998). Osteoprotegerin mRNA is expressed in primary human osteoblast-like cells: down-regulation by glucocorticoids. *J. Endocrinol.* **159**, 191-195.
Vindevoghel, L., Lechleider, R. J., Kon, A., de Caestecker, M. P., Uitto, J., Roberts, A. B. and Mauviel, A. (1998). SMAD3/4-dependent transcriptional activation of the human type VII collagen gene (COL7A1) promoter by transforming growth factor beta. *Proc. Natl. Acad. Sci. USA* **95**, 14769-14774.
Vrancken Peeters, M. P., Gittenberger-de Groot, A. C., Mentink, M. M. and Poelmann, R. E. (1999). Smooth muscle cells and fibroblasts of the coronary arteries derive from epithelial-mesenchymal transformation of the epicardium. *Anat. Embryol. (Berl.)* **199**, 367-378.
Wada, A. M., Reese, D. E. and Bader, D. M. (2001). Bves: prototype of a new class of cell adhesion molecules expressed during coronary artery development. *Development* **128**, 2085-2093.
Wilkins-Port, C. E. and Higgins, P. J. (2007). Regulation of extracellular matrix remodeling following transforming growth factor-beta1/epidermal growth factor-stimulated epithelial-mesenchymal transition in human premalignant keratinocytes. *Cells Tissues Organs* **185**, 116-122.
Xu, G. F., O'Connell, P., Viskochil, D., Cawthon, R., Robertson, M., Culver, M., Dunn, D., Stevens, J., Gesteland, R., White, R. et al. (1990). The neurofibromatosis type 1 gene encodes a protein related to GAP. *Cell* **62**, 599-608.
Xu, J., Ismat, F. A., Wang, T., Yang, J. and Epstein, J. A. (2007). NF1 regulates a Ras-dependent vascular smooth muscle proliferative injury response. *Circulation* **116**, 2148-2156.
Xu, J., Ismat, F. A., Wang, T., Lu, M. M., Antonucci, N. and Epstein, J. A. (2009a). Cardiomyocyte-specific loss of neurofibromin promotes cardiac hypertrophy and dysfunction. *Circ. Res.* **105**, 304-311.
Xu, J., Lamouille, S. and Derynck, R. (2009b). TGF-beta-induced epithelial to mesenchymal transition. *Cell Res.* **19**, 156-172.
Yang, J. and Weinberg, R. A. (2008). Epithelial-mesenchymal transition: at the crossroads of development and tumor metastasis. *Dev. Cell* **14**, 818-829.
Zhou, B., Ma, Q., Rajagopal, S., Wu, S. M., Domian, I., Rivera-Feliciano, J., Jiang, D., von Gise, A., Ikeda, S., Chien, K. R. et al. (2008). Epicardial progenitors contribute to the cardiomyocyte lineage in the developing heart. *Nature* **454**, 109-113.
Zhu, Y., Romero, M. I., Ghosh, P., Ye, Z., Charnay, P., Rushing, E. J., Marth, J. D. and Parada, L. F. (2001). Ablation of NF1 function in neurons induces abnormal development of cerebral cortex and reactive gliosis in the brain. *Genes Dev.* **15**, 859-876.
Zhu, Y., Ghosh, P., Charnay, P., Burns, D. K. and Parada, L. F. (2002). Neurofibromas in NF1: Schwann cell origin and role of tumor environment. *Science* **296**, 920-922.